FERMILAB–PUB–94/032–T

hep-ph/9402210

Mesons with Beauty and Charm: Spectroscopy

Estia J. Eichten* and Chris Quigg†

Theoretical Physics Department

Fermi National Accelerator Laboratory

P.O. Box 500, Batavia, Illinois 60510

(January 21, 1998)

Abstract

Applying knowledge of the interaction between heavy quarks derived from the study of $c\bar{c}$ and $b\bar{b}$ bound states, we calculate the spectrum of $c\bar{b}$ mesons. We compute transition rates for the electromagnetic and hadronic cascades that lead from excited states to the $^1S_0$ ground state, and briefly consider the prospects for experimental observation of the spectrum.

PACS numbers: 14.40Lb, 14.40Nd, 13.40Hq, 13.25-k

*Internet address: eichten@fnal.gov

†Internet address: quigg@fnal.gov

I. INTRODUCTION

The copious production of b quarks in Z^0 decays at the Large Electron-Positron collider (LEP) and in 1.8-TeV proton-antiproton collisions at the Fermilab Tevatron opens for study the rich spectroscopy of mesons and baryons beyond B_u^+ and B_d^0. In addition to B_s^0 and Λ_b^0, which have already been widely discussed, a particularly interesting case is the spectrum of $c\bar{b}$ states and its ground state, the B_c^+ meson [1].

Even more than their counterparts in the J/ψ and Υ families, the $c\bar{b}$ states that lie below the (BD) threshold for decay into a pair of heavy-flavored mesons are stable against strong decay, for they cannot annihilate into gluons. Their allowed decays, by E1 or M1 transitions or by hadronic cascades, lead to total widths that are less than a few hundred keV. All decay chains ultimately reach the $^1\mathrm{S}_0$ ground state B_c, which decays weakly. It may be possible, in time, to map out the excitation spectrum by observing photons or light hadrons in coincidence with a prominent decay of the B_c [2]. This would test our understanding of the force between heavy quarks.

The weak decays of the $c\bar{b}$ ground state will be of particular interest because the influence of the strong interaction can be estimated reliably [3]. The deep binding of the heavy quarks within the B_c means that the spectator picture is misleading. Taking proper account of binding energy, we expect a rather long lifetime that implies easily observable secondary vertices. The deep binding also affects the B_c branching fractions and leads us to expect that final states involving ψ will be prominent. The modes $\psi\pi^+$, ψa_1^+, $\psi\rho^+$, ψD_s^+, and $\psi\ell^+\nu_\ell$ will serve to identify B_c mesons and determine the B_c mass and lifetime.

In this Article, we present a comprehensive portrait of the spectroscopy of the B_c meson and its long-lived excited states. In Section II, we estimate the mass of the B_c in the framework of nonrelativistic quarkonium quantum mechanics and calculate the spectrum of $c\bar{b}$ states in detail. In Section III, we compute rates for the prominent radiative decays of the excited states and estimate rates and spectra of the hadronic cascades $(c\bar{b})_i \rightarrow \pi\pi + (c\bar{b})_f$ and $(c\bar{b})_i \rightarrow \eta + (c\bar{b})_f$. Using this information, we outline a strategy for partially reconstructing the $c\bar{b}$ spectrum. A brief summary appears in Section IV.

II. THE SPECTRUM OF B_c STATES

A. The Mass of B_c

Both in mass and in size, the mesons with beauty and charm are intermediate between the $c\bar{c}$ and $b\bar{b}$ states. Estimates of the B_c mass can, consequently, be tied to what is known about the charmonium and Υ families. To predict the full spectrum and properties of $c\bar{b}$ states, we rely on the nonrelativistic potential-model description of quarkonium levels. The interquark potential is known rather accurately in the region of space important for the J/ψ and Υ families [4–6], which spans the distances important for $c\bar{b}$ levels. This region lies between the short-distance Coulombic and long-distance linear behavior expected in QCD. We consider four functional forms for the potential that give reasonable accounts of the $c\bar{c}$ and $b\bar{b}$ spectra: the QCD-motivated potential [7] given by Buchmüller and Tye [8], with

$$m_c = 1.48\ \text{GeV}/c^2 \quad m_b = 4.88\ \text{GeV}/c^2 \ \ ; \tag{2.1}$$

a power-law potential [9],

$$V(r) = -8.064\ \text{GeV} + (6.898\ \text{GeV})(r \cdot 1\ \text{GeV})^{0.1} \ \ , \tag{2.2}$$

with

$$m_c = 1.8\ \text{GeV}/c^2 \quad m_b = 5.174\ \text{GeV}/c^2 \ \ ; \tag{2.3}$$

a logarithmic potential [10],

$$V(r) = -0.6635\ \text{GeV} + (0.733\ \text{GeV}) \log{(r \cdot 1\ \text{GeV})} \ \ , \tag{2.4}$$

with

$$m_c = 1.5\ \text{GeV}/c^2 \quad m_b = 4.906\ \text{GeV}/c^2 \ \ ; \tag{2.5}$$

and a Coulomb-plus-linear potential (the "Cornell potential") [4],

$$V(r) = -\frac{\kappa}{r} + \frac{r}{a^2} \quad , \tag{2.6}$$

with

$$m_c = 1.84\ \text{GeV}/c^2 \quad m_b = 5.18\ \text{GeV}/c^2 \tag{2.7}$$

$$\kappa = 0.52 \quad a = 2.34\ \text{GeV}^{-1} \quad . \tag{2.8}$$

We solve the Schrödinger equation for each of the potentials to determine the position of the 1S center of gravity for $c\bar{c}$, $c\bar{b}$, and $b\bar{b}$. The ${}^3\text{S}_1 - {}^1\text{S}_0$ splitting of the $i\bar{\jmath}$ ground state is given by

$$M({}^3\text{S}_1) - M({}^1\text{S}_0) = \frac{32\pi\alpha_s|\Psi(0)|^2}{9m_i m_j} \quad . \tag{2.9}$$

The hyperfine splitting observed in the charmonium family [1],

$$M(J/\psi) - M(\eta_c) = 117\ \text{MeV}/c^2 \quad , \tag{2.10}$$

fixes the strong coupling constant for each potential. We neglect the variation of α_s with momentum and scale the splitting of $c\bar{b}$ and $b\bar{b}$ from the charmonium value (2.10). The resulting values of vector and pseudoscalar masses are presented in Table I. Predictions for the $c\bar{b}$ ground-state masses depend little on the potential. The B_c and B_c^* masses and splitting lie within the ranges quoted by Kwong and Rosner [11] in their survey of techniques for estimating the masses of the $c\bar{b}$ ground state. They find

$$6.194\ \text{GeV}/c^2 \lesssim M_{B_c} \lesssim 6.292\ \text{GeV}/c^2 \quad , \tag{2.11}$$

and

$$6.284\ \text{GeV}/c^2 \lesssim M_{B_c^*} \lesssim 6.357\ \text{GeV}/c^2 \quad , \tag{2.12}$$

with

$$65\ \text{MeV}/c^2 \lesssim M_{B_c^*} - M_{B_c} \lesssim 90\ \text{MeV}/c^2 \quad . \tag{2.13}$$

We take

$$M_{B_c} = 6.258 \pm 0.020 \text{ GeV}/c^2 \tag{2.14}$$

as our best guess for the interval in which B_c will be found [12].

We shall adopt the Buchmüller-Tye potential [8] for the detailed calculations that follow, because it has the correct two-loop short-distance behavior in perturbative QCD.

B. Excited States

The interaction energies of a heavy quark-antiquark system probe the basic dynamics of the strong interaction. The gross structure of the quarkonium spectrum reflects the shape of the interquark potential. In the absence of light quarks, the static energy explicitly exhibits linear confinement at large distance. Further insight can be obtained by studying the spin-dependent forces, which distinguish the electric and magnetic parts of the interactions. Within the framework of quantum chromodynamics, the nature of the spin-dependent forces was first studied nonperturbatively by Eichten and Feinberg [13,14]. Gromes [15] subsequently added an important constraint that arises from boost-invariance of the QCD forms [16]. One-loop perturbative QCD calculations for the spin-dependent interactions in a meson composed of two different heavy quarks have also been carried out [17–19].

The spin-dependent contributions to the $c\bar{b}$ masses may be written as

$$\Delta = \sum_{k=1}^{4} T_k \quad , \tag{2.15}$$

where the individual terms are

$$\begin{aligned}
T_1 &= \frac{\langle \vec{L} \cdot \vec{s}_i \rangle}{2m_i^2} \tilde{T}_1(m_i, m_j) + \frac{\langle \vec{L} \cdot \vec{s}_j \rangle}{2m_j^2} \tilde{T}_1(m_j, m_i) \\
T_2 &= \frac{\langle \vec{L} \cdot \vec{s}_i \rangle}{m_i m_j} \tilde{T}_2(m_i, m_j) + \frac{\langle \vec{L} \cdot \vec{s}_j \rangle}{m_i m_j} \tilde{T}_2(m_j, m_i) \\
T_3 &= \frac{\langle \vec{s}_i \cdot \vec{s}_j \rangle}{m_i m_j} \tilde{T}_3(m_i, m_j) \\
T_4 &= \frac{\langle S_{ij} \rangle}{m_i m_j} \tilde{T}_4(m_i, m_j) \quad ,
\end{aligned} \tag{2.16}$$

and the tensor operator is

$$S_{ij} = 4\left[3(\vec{s}_i \cdot \hat{n})(\vec{s}_j \cdot \hat{n}) - \vec{s}_i \cdot \vec{s}_j\right] \quad . \tag{2.17}$$

In Eq. (2.16) and (2.17), $\vec{s}_i$ and $\vec{s}_j$ are the spins of the heavy quarks, $\vec{L}$ is the orbital angular momentum of quark and antiquark in the bound state, and $\hat{n}$ is an arbitrary unit vector. The total spin is $\vec{S} = \vec{s}_i + \vec{s}_j$.

The leading contributions to the $\tilde{T}_k$ have no explicit dependence on the quark masses. Assuming that the magnetic interactions are short-range ($\propto \langle r^{-3} \rangle$) and thus can be calculated in perturbation theory, we have

$$\begin{aligned}
\tilde{T}_1(m_i, m_j) &= -\left\langle \frac{1}{r}\frac{dV}{dR} \right\rangle + 2\tilde{T}_2(m_i, m_j) \\
\tilde{T}_2(m_i, m_j) &= \frac{4\alpha_s}{3}\langle r^{-3} \rangle \\
\tilde{T}_3(m_i, m_j) &= \frac{32\pi\alpha_s}{9}|\Psi(0)|^2 \\
\tilde{T}_4(m_i, m_j) &= \frac{\alpha_s}{3}\langle r^{-3} \rangle \; .
\end{aligned} \tag{2.18}$$

The connection between $\tilde{T}_1$ and $\tilde{T}_2$ is Gromes's general relation; the other equations reflect the stated approximations.

For quarkonium systems composed of equal-mass heavy quarks, the total spin S is a good quantum number and LS coupling leads to the familiar classification of states as ${}^{2S+1}L_J$, where $\vec{J} = \vec{L} + \vec{S}$ [20]. The calculated spectra are compared with experiment in Table II (for the ψ family) and Table III (for the Υ family). Overall, the agreement is satisfactory. Typical deviations in the charmonium system are less than about 30 MeV; deviations in the upsilon system are somewhat smaller. The differences between calculated and observed spectra suggest that the excitation energies in the $c\bar{b}$ system can be predicted within a few tens of MeV.

The leptonic decay rate of a neutral $(Q\bar{Q})$ vector meson V^0 is related to the Schrödinger wave function through [23,24]

$$\Gamma(V^0 \to e^+e^-) = \frac{16\pi N_c \alpha^2 e_Q^2}{3}\frac{|\Psi(0)|^2}{M_V^2}\left(1 - \frac{16\alpha_s}{3\pi}\right) \quad , \tag{2.19}$$

where $N_c = 3$ is the number of quark colors, e_Q is the heavy-quark charge, and M_V is the mass of the vector meson. The resulting leptonic widths, evaluated without QCD corrections, are tabulated in Tables II and III. Within each family, the leptonic widths are predicted in proper proportions, but are larger than the observed values. The QCD correction reduces the magnitudes significantly; the amount of this reduction is somewhat uncertain, because the first term in the perturbation expansion is large [25].

For unequal-mass quarks, it is more convenient to construct the mass eigenstates by jj coupling, first coupling $\vec{L}+\vec{s}_c = \vec{J}_c$ and then adding the spin of the heavier quark, $\vec{s}_b+\vec{J}_c = \vec{J}$. The level shifts $\Delta^{(J)}$ for the $L = 1$ states with $(J_c = \frac{3}{2}, J = 2)$ and $(J_c = \frac{1}{2}, J = 0)$ are

$$\begin{aligned} \Delta^{(2)} &= \left(\frac{1}{4m_c^2} + \frac{1}{4m_b^2}\right)\tilde{T}_1 + \frac{1}{m_b m_c}\tilde{T}_2 - \frac{2}{5m_b m_c}\tilde{T}_4 \\ \Delta^{(0)} &= -\left(\frac{1}{2m_c^2} + \frac{1}{2m_b^2}\right)\tilde{T}_1 - \frac{2}{m_b m_c}\tilde{T}_2 - \frac{4}{m_b m_c}\tilde{T}_4 \ . \end{aligned} \tag{2.20}$$

For a given principal quantum number, the two $(L = 1, J = 1)$ $c\bar{b}$ states with $J_c = \frac{1}{2}$ and $\frac{3}{2}$ are mixed in general. The elements of the mixing matrix are

$$\begin{aligned} \Delta^{(1)}_{\frac{3}{2}\frac{3}{2}} &= \left(\frac{1}{4m_c^2} - \frac{5}{12m_b^2}\right)\tilde{T}_1 - \frac{1}{3m_b m_c}\tilde{T}_2 + \frac{2}{3m_b m_c}\tilde{T}_4 \\ \Delta^{(1)}_{\frac{3}{2}\frac{1}{2}} = \Delta^{(1)}_{\frac{1}{2}\frac{3}{2}} &= -\frac{\sqrt{2}}{6m_b^2}\tilde{T}_1 - \frac{\sqrt{2}}{3m_b m_c}\tilde{T}_2 + \frac{2\sqrt{2}}{3m_b m_c}\tilde{T}_4 \\ \Delta^{(1)}_{\frac{1}{2}\frac{1}{2}} &= \left(-\frac{1}{2m_c^2} + \frac{1}{6m_b^2}\right)\tilde{T}_1 - \frac{2}{3m_b m_c}\tilde{T}_2 + \frac{4}{3m_b m_c}\tilde{T}_4 \ . \end{aligned} \tag{2.21}$$

Two limiting cases are familiar.

(i) With equal quark masses $m_b = m_c \equiv m$, the level shifts become

$$\begin{aligned} \Delta^{(2)} &= \frac{1}{2m^2}\tilde{T}_1 + \frac{1}{m^2}\tilde{T}_2 - \frac{2}{5m^2}\tilde{T}_4 \\ \Delta^{(0)} &= -\frac{1}{m^2}\tilde{T}_1 - \frac{2}{m^2}\tilde{T}_2 - \frac{4}{m^2}\tilde{T}_4 \ , \end{aligned} \tag{2.22}$$

while the mixing matrix becomes

$$\Delta^{(1)} = \begin{pmatrix} 1 & \sqrt{2} \\ \sqrt{2} & 2 \end{pmatrix} \left(\frac{-\tilde{T}_1 - 2\tilde{T}_2 + 4\tilde{T}_4}{6m^2}\right) \ . \tag{2.23}$$

The mass eigenstates are the familiar ^{1}P$_1$ and ^{3}P$_1$ states of the LS coupling scheme. In this basis, they may be written as

$$
\begin{aligned}
|^1\mathrm{P}_1\rangle &= -\sqrt{\tfrac{2}{3}}|J_c=\tfrac{3}{2}\rangle + \sqrt{\tfrac{1}{3}}|J_c=\tfrac{1}{2}\rangle \\
|^3\mathrm{P}_1\rangle &= \sqrt{\tfrac{1}{3}}|J_c=\tfrac{3}{2}\rangle + \sqrt{\tfrac{2}{3}}|J_c=\tfrac{1}{2}\rangle
\end{aligned}
\tag{2.24}
$$

with eigenvalues

$$
\begin{pmatrix} \lambda(^1\mathrm{P}_1) \\ \lambda(^3\mathrm{P}_1) \end{pmatrix} = \begin{pmatrix} 0 \\ 3 \end{pmatrix} \left(\frac{-\tilde{T}_1 - 2\tilde{T}_2 + 4\tilde{T}_4}{6m^2} \right) \quad . \tag{2.25}
$$

The position of the ^{1}P$_1$ level coincides with the centroid $[5\Delta^{(2)} + 3\lambda(^3\mathrm{P}_1) + \Delta^{(0)}]/9$ of the ^{3}P$_J$ levels.

(ii) In the heavy-quark limit, $m_b \to \infty$, the level shifts of the $J = 0, 2$ levels become

$$
\begin{aligned}
\Delta^{(2)} &= \frac{1}{4m_c^2}\tilde{T}_1 \\
\Delta^{(0)} &= -\frac{1}{2m_c^2}\tilde{T}_1 \quad ,
\end{aligned}
\tag{2.26}
$$

while the mixing matrix becomes

$$
\Delta^{(1)} = \begin{pmatrix} 1 & 0 \\ 0 & -2 \end{pmatrix} \left(\frac{\tilde{T}_1}{4m_c^2} \right) \quad . \tag{2.27}
$$

The $J_c = \frac{3}{2}$ and $J_c = \frac{1}{2}$ states separate into degenerate pairs, as expected on the basis of heavy-quark symmetry [26].

In the $c\bar{b}$ system, we label the mass eigenstates obtained by diagonalizing the matrix (2.21) as $n(1^+)$ and $n(1^{+\prime})$. For the 2P$_1$ levels, the mixing matrix is

$$
\Delta^{(2\mathrm{P})} = \begin{pmatrix} -1.85 & -2.80 \\ -2.80 & -4.23 \end{pmatrix} \ \mathrm{MeV} \quad , \tag{2.28}
$$

with eigenvectors

$$
\begin{aligned}
|2(1^+)\rangle &= 0.552|J_c=\tfrac{3}{2}\rangle + 0.833|J_c=\tfrac{1}{2}\rangle \\
|2(1^{+\prime})\rangle &= -0.833|J_c=\tfrac{3}{2}\rangle + 0.552|J_c=\tfrac{1}{2}\rangle
\end{aligned}
\tag{2.29}
$$

and eigenvalues

$$\lambda_2 = -6.09 \text{ MeV} \tag{2.30}$$
$$\lambda_2' = 0.00057 \text{ MeV} \quad .$$

For the 3P$_1$ levels, the mixing matrix is

$$\Delta^{(3\mathrm{P})} = \begin{pmatrix} -0.13 & -2.54 \\ -2.54 & -6.91 \end{pmatrix} \text{ MeV} \quad , \tag{2.31}$$

with eigenvectors

$$|3(1^+)\rangle = 0.316|J_c = \tfrac{3}{2}\rangle + 0.949|J_c = \tfrac{1}{2}\rangle \tag{2.32}$$
$$|3(1^{+\prime})\rangle = -0.949|J_c = \tfrac{3}{2}\rangle + 0.316|J_c = \tfrac{1}{2}\rangle$$

and eigenvalues

$$\lambda_3 = -7.76 \text{ MeV} \tag{2.33}$$
$$\lambda_3' = 0.711 \text{ MeV} \quad .$$

For the 4P$_1$ levels, the mixing matrix is

$$\Delta^{(4\mathrm{P})} = \begin{pmatrix} 0.71 & -2.44 \\ -2.44 & -8.31 \end{pmatrix} \text{ MeV} \quad , \tag{2.34}$$

with eigenvectors

$$|4(1^+)\rangle = 0.245|J_c = \tfrac{3}{2}\rangle + 0.969|J_c = \tfrac{1}{2}\rangle \tag{2.35}$$
$$|4(1^{+\prime})\rangle = -0.969|J_c = \tfrac{3}{2}\rangle + 0.245|J_c = \tfrac{1}{2}\rangle$$

and eigenvalues

$$\lambda_4 = -8.93 \text{ MeV} \tag{2.36}$$
$$\lambda_4' = 1.32 \text{ MeV} \quad .$$

The calculated spectrum of $c\bar{b}$ states is presented in Table IV and Figure 1. Our spectrum is similar to others calculated by Eichten and Feinberg [14] in the Cornell potential [4], by

Gershteĭn et al. [27] in the power-law potential (2.2), and by Chen and Kuang [28] in their own version of a QCD-inspired potential. Levels that lie below the BD flavor threshold, i.e., with $M < M_D + M_B = 7.1431 \pm 0.0021$ GeV/c^2, will be stable against fission into heavy-light mesons.

C. Properties of $c\bar{b}$ Wave Functions at the Origin

For quarks bound in a central potential, it is convenient to separate the Schrödinger wave function into radial and angular pieces, as

$$\Psi_{n\ell m}(\vec{r}) = R_{n\ell}(r) Y_{\ell m}(\theta, \phi) \quad , \tag{2.37}$$

where n is the principal quantum number, ℓ and m are the orbital angular momentum and its projection, $R_{n\ell}(r)$ is the radial wave function, and $Y_{\ell m}(\theta, \phi)$ is a spherical harmonic [29]. The Schrödinger wave function is normalized,

$$\int d^3\vec{r} |\Psi_{n\ell m}(\vec{r})|^2 = 1 \quad , \tag{2.38}$$

so that

$$\int_0^\infty r^2 dr |R_{n\ell}(r)| = 1 \quad . \tag{2.39}$$

The value of the radial wave function, or its first nonvanishing derivative at the origin,

$$R_{n\ell}^{(\ell)}(0) \equiv \left. \frac{d^\ell R_{n\ell}(r)}{dr^\ell} \right|_{r=0} \quad , \tag{2.40}$$

is required to evaluate pseudoscalar decay constants and production rates through heavy-quark fragmentation [30]. The quantity $|R_{n\ell}^{(\ell)}(0)|^2$ is presented for four potentials in Table V. The stronger singularity of the Cornell potential is reflected in spatially smaller states.

The pseudoscalar decay constant f_{B_c}, which will be required for the discussion of annihilation decays $c\bar{b} \to W^+ \to$ final state, is defined by

$$\langle 0 | A_\mu(0) | B_c(q) \rangle = i f_{B_c} V_{cb} q_\mu \quad , \tag{2.41}$$

where A_μ is the axial-vector part of the charged weak current, V_{cb} is an element of the Cabibbo-Kobayashi-Maskawa quark-mixing matrix, and q_μ is the four-momentum of the B_c. The pseudoscalar decay constant is related to the ground-state $c\bar{b}$ wave function at the origin by the van Royen-Weisskopf formula [23] modified for color,

$$f_{B_c}^2 = \frac{12|\Psi_{100}(0)|^2}{M} = \frac{3|R_{10}(0)|^2}{\pi M} \quad . \tag{2.42}$$

In the nonrelativistic potential models we have considered to estimate M_{B_c} and $M_{B_c^*}$, we find

$$f_{B_c} = \begin{cases} 500 \text{ MeV (Buchmüller-Tye potential [8])} \\ 512 \text{ MeV (power-law potential [9])} \\ 479 \text{ MeV (logarithmic potential [10])} \\ 687 \text{ MeV (Cornell potential [4]).} \end{cases} \tag{2.43}$$

Even after QCD radiative corrections of the size suggested by the comparison of computed and observed leptonic widths for J/ψ and Υ, f_{B_c} will be significantly larger than the pion decay constant, $f_\pi = 131.74 \pm 0.15$ MeV [1]. The compact size of the $c\bar{b}$ system enhances the importance of annihilation decays.

III. TRANSITIONS BETWEEN $c\bar{b}$ STATES

As in atomic physics, it is the spectral lines produced in cascades from excited states to the readily observable B_c ground state that will reveal the $c\bar{b}$ level scheme. As in the J/ψ and Υ quarkonium families, the transitions are mostly radiative decays. A few hadronic cascades, analogs of the $2^3\text{S}_1 \to 1^3\text{S}_1\pi\pi$ transition first observed in charmonium, will also be observable.

A. Electromagnetic Transitions

Except for the magnetic-dipole (spin-flip) transition between the ground-state B_c^* and B_c, only the electric dipole transitions are important for mapping the $c\bar{b}$ spectrum.

1. Electric Dipole Transitions

The strength of the electric-dipole transitions is governed by the size of the radiator and the charges of the constituent quarks. The E1 transition rate is given by

$$\Gamma_{\mathrm{E1}}(i \to f + \gamma) = \frac{4\alpha < e_Q >^2}{27} k^3 (2J_f + 1) |\langle f|r|i\rangle|^2 \mathcal{S}_{if} \quad , \tag{3.1}$$

where the mean charge is

$$< e_Q > = \frac{m_b e_c - m_c e_{\bar{b}}}{m_b + m_c} \quad , \tag{3.2}$$

k is the photon energy, and the statistical factor $\mathcal{S}_{if} = \mathcal{S}_{fi}$ is as defined by Eichten and Gottfried [31]. $\mathcal{S}_{if} = 1$ for ${}^3\mathrm{S}_1 \to {}^3\mathrm{P}_J$ transitions and $\mathcal{S}_{if} = 3$ for allowed E1 transitions between spin-singlet states. The statistical factors for d-wave to p-wave transitions are reproduced in Table VI for convenience. The E1 transition rates and photon energies in the $c\bar{b}$ system are presented in Table VII.

2. Magnetic Dipole Transitions

The only decay mode for the $1^3\mathrm{S}_1$ (B_c^*) state is the magnetic dipole transition to the ground state, B_c. The M1 rate for transitions between s-wave levels is given by

$$\Gamma_{\mathrm{M1}}(i \to f + \gamma) = \frac{16\alpha}{3} \mu^2 k^3 (2J_f + 1) |\langle f|j_0(kr/2)|i\rangle|^2 \quad , \tag{3.3}$$

where the magnetic dipole moment is

$$\mu = \frac{m_b e_c - m_c e_{\bar{b}}}{4 m_c m_b} \tag{3.4}$$

and k is the photon energy. Rates for the allowed and hindered M1 transitions between spin-triplet and spin-singlet s-wave $c\bar{b}$ states are given in Table VIII. The M1 transitions contribute little to the total widths of the 2S levels. Because it cannot decay by annihilation, the $1^3\mathrm{S}_1$ $c\bar{b}$ level, with a total width of 135 eV, is far more stable than its counterparts in the $c\bar{c}$ and $b\bar{b}$ systems, whose total widths are 68 ± 10 keV and 52.1 ± 2.1 keV, respectively [1].

B. Hadronic Transitions

A hadronic transition between quarkonium levels can be understood as a two-step process in which gluons first are emitted from the heavy quarks and then recombine into light hadrons. Perturbative QCD is not directly applicable, because the energy available to the light hadrons is small and the emitted gluons are soft. Nevertheless, the final quarkonium state is small compared to the system of light hadrons and moves nonrelativistically in the rest frame of the decaying quarkonium state. A multipole expansion of the color gauge field converges rapidly and leads to selection rules, a Wigner-Eckart theorem, and rate estimates for hadronic transitions [32]. The recombination of gluons into light hadrons involves the full strong dynamics and can only be modeled. The general structure of hadronic-cascade transitions and models for the recombination of gluons into light hadrons can be found in a series of papers by Yan and collaborators [33–36].

The hadronic transition rates for an unequal-mass $Q\bar{Q}'$ system differ in some details from the rates for an equal-mass $Q\bar{Q}$ system with the same reduced mass. The relative strengths of various terms that contribute to magnetic-multipole transitions are modified because of the unequal quark and antiquark masses. The electric-multipole transitions are only sensitive to the relative position of the quark and antiquark and will be unchanged in form.

As in the $c\bar{c}$ and $b\bar{b}$ systems, the principal hadronic transitions in the $c\bar{b}$ system involve the emission of two pions. Electric-dipole contributions dominate in these transitions, and so the equal-mass results apply directly. The initial quarkonium state is characterized by its total angular momentum J' with z-component M', orbital angular momentum ℓ', spin s', and other quantum numbers collectively labelled by α'. The corresponding quantum numbers of the final quarkonium state are denoted by the unprimed symbols. Since the transition operator is spin-independent, the initial and final spins are the same: $s' = s$. Because the gauge-field operators in the transition amplitude do not depend on the heavy-quark variables, the transition operator is a reducible second-rank tensor, which may be decomposed into a sum of irreducible tensors with rank $k = 0, 1, 2$. The differential rate [33] for the E1–E1 transition from the initial quarkonium state Φ' to the final quarkonium state Φ and a system of n light hadrons, denoted h, is given by

$$\frac{d\Gamma}{d\mathcal{M}^2}(\Phi' \to \Phi + h) = (2J+1) \sum_{k=0}^{2} \begin{Bmatrix} k & \ell' & \ell \\ s & J & J' \end{Bmatrix}^2 A_k(\ell', \ell) \ , \tag{3.5}$$

where $\mathcal{M}^2$ is the invariant mass squared of the light hadron system, $\{\ \}$ is a 6-j symbol, and $A_k(\ell', \ell)$ is the contribution of the irreducible tensor with rank k. The Wigner-Eckart theorem (3.5) yields the relations among two-pion transition rates given in Table IX.

The magnitudes of the $A_k(\ell', \ell)$ are model-dependent. Since the A_1 contributions are suppressed in the soft-pion limit [33], we will set $A_1(\ell', \ell) = 0$. For some of the remaining rates we can use simple scaling arguments from the measured rates in $Q\bar{Q}$ systems [37]. The amplitude for an E1–E1 transition depends quadratically on the interquark separation, so the scaling law between a $Q\bar{Q}'$ and the corresponding $Q\bar{Q}$ system states is given by [32,33]:

$$\frac{\Gamma(Q\bar{Q}')}{\Gamma(Q\bar{Q})} = \frac{\langle r^2(Q\bar{Q}')\rangle^2}{\langle r^2(Q\bar{Q})\rangle^2} \ , \tag{3.6}$$

up to possible differences in phase space. The measured values for the $\psi' \to \psi + \pi\pi$, $\Upsilon' \to \Upsilon + \pi\pi$, and $\psi(3770) \to \psi + \pi\pi$ transition rates allow good scaling estimates for the 2S $\to$ 1S + $\pi\pi$ and 3D $\to$ 1S + $\pi\pi$ transitions in the $c\bar{b}$ system. We have estimated the remaining transition rates by scaling the $b\bar{b}$ rates calculated by Kuang and Yan [34] in their Model C, which is based on the Buchmüller-Tye potential [8]. The results are shown in Table X.

Chiral symmetry leads to a universal form for the normalized dipion spectrum [41],

$$\frac{1}{\Gamma}\frac{d\Gamma}{d\mathcal{M}} = \text{Constant} \times \frac{|\vec{K}|}{M_{\Phi'}^2}(2x^2-1)^2\sqrt{x^2-1} \ , \tag{3.7}$$

where $x = \mathcal{M}/2m_\pi$ and

$$|\vec{K}| = \frac{\sqrt{M_{\Phi'}^2 - (\mathcal{M} + M_\Phi)^2}\sqrt{M_{\Phi'}^2 - (\mathcal{M} - M_\Phi)^2}}{2M_{\Phi'}} \tag{3.8}$$

is the three-momentum carried by the pion pair. The normalized invariant-mass distribution for the transition $2^3\mathrm{S}_1 \to 1^3\mathrm{S}_1 + \pi\pi$ is shown in Figure 2 for the $c\bar{c}$, $c\bar{b}$, and $b\bar{b}$ families. The soft-pion expression (3.7) describes the depletion of the dipion spectrum at low invariant masses observed in the transitions $\psi(2\mathrm{S}) \to \psi(1\mathrm{S})\pi\pi$ [42] and $\Upsilon(2\mathrm{S}) \to \Upsilon(1\mathrm{S})\pi\pi$ [43], but fails to account for the $\Upsilon(3\mathrm{S}) \to \Upsilon(1\mathrm{S})\pi\pi$ and $\Upsilon(3\mathrm{S}) \to \Upsilon(2\mathrm{S})\pi\pi$ spectra [44]. We expect the 3S levels to lie above flavor threshold in the $c\bar{b}$ system.

By the Wigner-Eckart theorem embodied in Eq. (3.5), the invariant mass spectrum in the decay $B_c(2\mathrm{S}) \to B_c(1\mathrm{S}) + \pi\pi$ should have the same form (3.7) as the $B_c^*(2\mathrm{S}) \to B_c^*(1\mathrm{S}) + \pi\pi$ transition. Braaten, Cheung, and Yuan [30] have calculated the probability for a high-energy $\bar{b}$ antiquark to fragment into the $c\bar{b}$ s-waves as 3.8×10^{-4} for $\bar{b} \to B_c(1\mathrm{S})$, 5.4×10^{-4} for $\bar{b} \to B_c^*(1\mathrm{S})$, 2.3×10^{-4} for $\bar{b} \to B_c(2\mathrm{S})$, and 3.2×10^{-4} for $\bar{b} \to B_c^*(2\mathrm{S})$. Given the excellent experimental signatures for $B_c(1\mathrm{S})$ decay and the favorable prospects for $B_c(2\mathrm{S})$ production in high-energy proton-antiproton collisions, it may be possible to observe the $0 \to 0$ transition for the first time in the B_c family.

The $2^3\mathrm{S}_1 \to 1^3\mathrm{S}_1 + \eta$ transition has been observed in charmonium. This transition proceeds via an M1–M1 or E1–M2 multipole. In the $c\bar{b}$ system the E1–M2 multipole dominates and the scaling from the $c\bar{c}$ system should be given by

$$\frac{\Gamma(c\bar{b})}{\Gamma(c\bar{c})} = \frac{(m_b+m_c)^2}{4m_b^2}\frac{\langle r^2(c\bar{b})\rangle}{\langle r^2(c\bar{c})\rangle}\frac{M_{\psi'}^3}{M_{\Phi'}^3}\frac{[M_{\Phi'}^2-(M_\Phi+M_\eta)^2]^{1/2}[M_{\Phi'}^2-(M_\Phi-M_\eta)^2]^{1/2}}{[M_{\psi'}^2-(M_\psi+M_\eta)^2]^{1/2}[M_{\psi'}^2-(M_\psi-M_\eta)^2]^{1/2}}\ , \quad (3.9)$$

where $M_{\Phi'}$ and M_Φ are the masses of the $2^3\mathrm{S}_1$ and $1^3\mathrm{S}_1$ $c\bar{b}$ levels, respectively. Because of the small energy release in this transition, the slightly smaller level spacing in the B_c family compared to the J/ψ family (562 MeV *vs.* 589 MeV) strongly suppresses η-emission in the $c\bar{b}$ system. The observed rate of $\Gamma(\psi' \to \psi + \eta) = 6.6 \pm 2.1$ keV [1] scales to $\Gamma(B_c(2\mathrm{S}) \to B_c(1\mathrm{S}) + \eta) = 0.25$ keV.

C. Total Widths and Experimental Signatures

The total widths and branching fractions are given in Table XI. The most striking feature of the $c\bar{b}$ spectrum is the extreme narrowness of the states. A crucial element in unraveling the spectrum will be the efficient detection of the 72-MeV M1-photon that, in coincidence with an observed B_c decay, tags the B_c^*. This will be essential for distinguishing the $B_c(2S) \to B_c(1S) + \pi\pi$ transition from $B_c^*(2S) \to B_c^*(1S) + \pi\pi$, which will have a nearly identical spectrum and a comparable rate. Combining the branching fractions in Table XI with the b-quark fragmentation probabilities of Ref. [30], we expect the cross section times branching fractions to be in the proportions

$$\sigma B(B_c(2S) \to B_c(1S) + \pi\pi) \approx 1.2 \times \sigma B(B_c^*(2S) \to B_c^*(1S) + \pi\pi) \ . \tag{3.10}$$

A reasonable—but challenging—experimental goal would be to map the eight lowest-lying $c\bar{b}$ states: the 1S, 2S, and 2P levels. A first step, in addition to reconstructing the hadronic cascades we have just discussed, would be the detection of the 455-MeV photons in coincidence with B_c, and of 353-, 382-, and 397-MeV photons in coincidence with $B_c^* \to B_c + \gamma(72\text{ MeV})$. This would be a most impressive triumph of experimental art.

IV. CONCLUDING REMARKS

A meson with beauty and charm is an exotic particle, but prospects are good that it will be discovered in the near future. As soon as B_c has been identified, the investigation of competing weak-decay mechanisms, $\bar{b} \to \bar{c}W^+$ (represented by $\psi\pi^+$, $\psi\ell^+\nu$, etc.), $c \to sW^+$ (represented by $B_s\pi^+$, $B_s\ell^+\nu$, etc.), and $c\bar{b} \to W^+$ (represented by ψD_s^+, $\tau^+\nu_\tau$, etc.), can begin. The issues to be studied, and predictions for a wide variety of inclusive and exclusive decays, are presented in a companion paper [3]. Before the end of the decade, it should prove possible to map out part of the $c\bar{b}$ spectrum by observing γ- and $\pi\pi$-coincidences with the ground-state B_c or its hyperfine partner B_c^*.

ACKNOWLEDGMENTS

Fermilab is operated by Universities Research Association, Inc., under contract DE-AC02-76CHO3000 with the United States Department of Energy. C.Q. thanks the Cultural

Section of the Vienna municipal government and members of the Institute for Theoretical Physics of the University of Vienna for their warm hospitality while part of this work was carried out.

REFERENCES

[1] We follow the nomenclature of the Particle Data Group, in which B mesons contain $\bar{b}$ antiquarks. See Particle Data Group, Phys. Lett. B **239,** 1 (1990); Phys. Rev. D **45,** S1 (1992).

[2] The CDF Collaboration has reconstructed the χ_c states by observing photons in coincidence with leptonic decays of J/ψ. See F. Abe *et al.* (CDF Collaboration), Phys. Rev. Lett. **71,** 2537 (1993).

[3] E. Eichten and C. Quigg, in preparation. For a brief preliminary account, see C. Quigg, FERMILAB-CONF-93/265–T, contributed to the Workshop on B Physics at Hadron Accelerators, Snowmass.

[4] E. Eichten, K. Gottfried, T. Kinoshita, K. D. Lane, T.-M. Yan, Phys. Rev. D **17,** 3090 (1978); ibid. **21,** 313(E) (1980); ibid. **21,** 203 (1980).

[5] C. Quigg and J. L. Rosner, Phys. Rev. D **23,** 2625 (1981).

[6] W. Kwong, J. L. Rosner, and C. Quigg, Ann. Rev. Nucl. Part. Sci. **37,** 325 (1987).

[7] J. Richardson, Phys. Lett. B **82,** 272 (1979).

[8] W. Buchmüller and S.-H. H. Tye, Phys. Rev. D **24,** 132 (1981).

[9] A. Martin, Phys. Lett. B **93,** 338 (1980); in *Heavy Flavours and High Energy Collisions in the 1-100 TeV Range,* edited by A. Ali and L. Cifarelli (Plenum Press, New York, 1989), p. 141.

[10] C. Quigg and J. L. Rosner, Phys. Lett. B **71,** 153 (1977).

[11] W. Kwong and J. L. Rosner, Phys. Rev. D **44,** 212 (1991).

[12] M. Baker, J. S. Ball, and F. Zachariasen, Phys. Rev. D **45,** 910 (1992), use a dual-QCD potential to calculate $M_{B_c} = 6.287$ GeV/c^2 and $M_{B_c^*} = 6.372$ GeV/c^2. We note that their prediction for the $(c\bar{c})$ 1S level lies at 3.083 GeV/c^2, 16 MeV/c^2 above the observed value.

R. Roncaglia, A. R. Dzierba, D. B. Lichtenberg, and E. Predazzi, Indiana University preprint IUHET 270 (January 1994, unpublished), use the Feynman-Hellman theorem to predict $M_{B_c^*} = 6.320 \pm 0.010$ GeV/c^2. S. Godfrey and N. Isgur, Phys. Rev. D **32,** 189 (1985), estimate $M_{B_c} = 6.27$ GeV/c^2 and $M_{B_c^*} = 6.34$ GeV/c^2.

[13] E. J. Eichten and F. Feinberg, Phys. Rev. Lett. **43,** 1205 (1979).

[14] E. J. Eichten and F. Feinberg, Phys. Rev. D **23,** 2724 (1981).

[15] D. Gromes, Z. Phys. C **26,** 401 (1984).

[16] General reviews of the Eichten-Feinberg-Gromes (EFG) formulation have been given by M. Peskin, in *Dynamics and Spectroscopy at High Energy,* Proceedings of the Eleventh SLAC Summer Institute on Particle Physics, SLAC Report No. 267, edited by P. M. McDonough (Stanford Linear Accelerator Center, Stanford, CA, 1983), p. 151; E. J. Eichten, in *The Sixth Quark,* Proceedings of the Twelfth SLAC Summer Institute on Particle Physics, SLAC Report No. 281, edited by P. M. McDonough (Stanford Linear Accelerator Center, Stanford, CA, 1985), p. 1. In Eq. (2.13), $V_2(R)$ should read $\dfrac{dV_2(R)}{dR}$; D. Gromes, in *Spectroscopy of Light and Heavy Quarks,* edited by Ugo Gastaldi, Robert Klapisch, and Frank Close (Plenum Press, New York and London, 1987), p. 67; D. Gromes, in *The Quark Structure of Matter,* Proceedings of the Yukon Advanced Study Institute, edited by N. Isgur, G. Karl, and P. J. O'Donnell (World Scientific, Singapore, 1985), p. 1.

[17] W. Buchmüller, Y. J. Ng, and S.-H. Henry Tye, Phys. Rev. D **24,** 3003 (1981).

[18] S. N. Gupta, S. F. Radford, and W. W. Repko, Phys. Rev. D **25,** 3430 (1982); ibid. **26,** 3305 (1982).

[19] For the unequal-mass case relevant to the $c\bar{b}$ system, Y. J. Ng, J. Pantaleone, and S.-H. Henry Tye, Phys. Rev. Lett. **55,** 916 (1985) [see also J. Pantaleone, S.-H. H. Tye, and Y. J. Ng, Phys. Rev. D **33,** 777 (1986)], introduced a new, spin-dependent form factor.

However, these changes can be absorbed into the EFG formalism without introducing any new form factors by allowing the existing form factor to depend (logarithmically) on the heavy-quark masses. Recently, Yu-Qi Chen and Yu-Ping Kuang, "General relations of heavy quark-antiquark potentials induced by reparametrization invariance," China Center of Advanced Science and Technology (World Laboratory) preprint CCAST-93-37 (unpublished), extended the Gromes analysis [15] to show in general that no new spin-dependent structures appear to order $1/m^2$.

[20] The expectation values of spin and orbital angular momentum operators are conveniently evaluated using $\langle \vec{s}_i \cdot \vec{s}_j \rangle = \frac{1}{2}S(S+1) - \frac{3}{4}$, $\langle \vec{L} \cdot \vec{s}_i \rangle = \langle \vec{L} \cdot \vec{s}_j \rangle = \frac{1}{2}\langle \vec{L} \cdot \vec{S} \rangle$, $\langle \vec{L} \cdot \vec{S} \rangle = \frac{1}{2}[J(J+1) - L(L+1) - S(S+1)]$. The tensor operator can be written as $S_{ij} = 2\left[3(\vec{S}\cdot\hat{n})(\vec{S}\cdot\hat{n}) - \vec{S}^2\right]$, for which [W. Kwong and J. L. Rosner, Phys. Rev. D **38,** 279 (1988)] $\langle S_{ij} \rangle = -[12\langle \vec{L}\cdot\vec{S}\rangle^2 + 6\langle \vec{L}\cdot\vec{S}\rangle - 4S(S+1)L(L+1)]/[(2L-1)(2L+3)]$.

[21] T. A. Armstrong *et al.* (E-760 Collaboration), Phys. Rev. Lett. **68,** 1468 (1992); Nucl. Phys. B **373,** 35 (1992).

[22] T. A. Armstrong *et al.* (E-760 Collaboration), Phys. Rev. Lett. **69,** 2337 (1992).

[23] Up to the color factor, this relation is due to R. Van Royen and V. F. Weisskopf, Nuovo Cim. **50,** 617 (1967); **51,** 583 (1967).

[24] The QCD radiative correction factor is obtained by transcription from QED. See, for example, R. Barbieri *et al.,* Nucl. Phys. **B105,** 125 (1976); W. Celmaster, Phys. Rev. D **19,** 1517 (1979).

[25] If, for example, we interpret the factor $(1 - 16\alpha_s/3\pi)$ as the beginning of an expansion for $(1 + 16\alpha_s/3\pi)^{-1}$ with $\alpha_s = 0.36$, then the predictions for the ψ family agree with experiment, within errors, while those for the Υ family are about 20% low.

[26] E. Eichten, K. Gottfried, T. Kinoshita, K. D. Lane, T.-M. Yan, Phys. Rev. D **21,** 203 (1980), observed in the context of potential models that, in the heavy-quark limit,

the state with $J_{\text{light quark}} = \frac{3}{2}$ is degenerate with the $^3\text{P}_2$ level, while the state with $J_{\text{light quark}} = \frac{1}{2}$ is degenerate with the $^3\text{P}_0$ level. (See their Appendix on charmed mesons.) See also J. L. Rosner, Comments Nucl. Part. Phys. **16,** 109 (1986). The observation in the heavy-quark limit of QCD is due to N. Isgur and M. B. Wise, Phys. Rev. Lett. **66,** 1130 (1991).

[27] S. S. Gershteĭn, V. V. Kiselev, A. K. Likhoded, S. R. Slabospitskiĭ, and A. V. Tkabladze, Yad. Fiz. **48,** 515 (1988); [Sov. J. Nucl. Phys. **48,** 327 (1988)].

[28] Yu-Qi Chen and Yu-Ping Kuang, Phys. Rev. D **46,** 1165 (1992). See also Yu-Qi Chen, "The Study of $B_c(\bar{B}_c)$ Meson and Its Excited States," Institute for Theoretical Physics, Academia Sinica, Ph.D. thesis, October 24, 1992 (unpublished).

[29] We adopt the standard normalization, $\int d\Omega\, Y^*_{\ell m}(\theta,\phi) Y_{\ell' m'}(\theta,\phi) = \delta_{\ell\ell'}\,\delta_{mm'}$. See, for example, the Appendix of Hans A. Bethe and Edwin E. Salpeter, *Quantum Mechanics of One- and Two-Electron Atoms* (Springer-Verlag, Berlin, 1957).

[30] Eric Braaten, Kingman Cheung, and Tzu Chiang Yuan, Phys. Rev. D **48,** R5049 (1993); Kingman Cheung, "B_c Meson Production at Hadron Colliders by Heavy Quark Fragmentation," NUHEP-TH-93-19 (unpublished); Yu-Qi Chen, "Perturbative QCD Predictions for the Fragmentation Functions of the P-Wave Mesons with Two Heavy Quarks," China Center for Advanced Science and Technology (World Laboratory) preprint CCAST-93-4 (unpublished).

[31] E. Eichten and K. Gottfried, Phys. Lett. B **66,** 286 (1977).

[32] K. Gottfried, in *Proceedings of the International Symposium on Lepton and Photon Interactions as High Energies,* edited by F. Gutbrod, DESY, Hamburg (1978); Phys. Rev. Lett. **40,** 598 (1978); M. B. Voloshin, Nucl. Phys. B **154,** 365 (1979).

[33] T.-M. Yan, Phys. Rev. D **22,** 1652 (1980).

[34] Y.-P. Kuang and T.-M. Yan, Phys. Rev. D **24,** 2874 (1981).

[35] Y.-P. Kuang, S. F. Tuan and T.-M. Yan, Phys. Rev. D **37,** 1210 (1988).

[36] Y.-P. Kuang and T.-M. Yan, Phys. Rev. D **41,** 155 (1990).

[37] It must be remembered in applying these relations to the $c\bar{b}$ system that the physical eigenstates with $J = \ell \neq 0$ are linear combinations of the equal-mass spin-singlet and spin-triplet states.

[38] R. A. Partridge, Ph. D. thesis, Caltech Report No. CALT-68-1150 (1984, unpublished).

[39] R. H. Schindler, Ph. D. thesis, Stanford Linear Accelerator Laboratory Report No. SLAC-219 (1979, unpublished).

[40] J. Adler, et al. (Mark III Collaboration), Phys. Rev. Lett. **60,** 89 (1988).

[41] L. S. Brown and R. N. Cahn, Phys. Rev. Lett. **35,** 1 (1975).

[42] G. S. Abrams *et al.* (Mark I Collaboration), Phys. Rev. Lett. **34,** 1181 (1975); G. S. Abrams, in *Proceedings of the 1975 International Symposium on Lepton and Photon Interactions at High Energies,* edited by W. T. Kirk (SLAC, Stanford, 1975), p. 25.

[43] D. Besson *et al.* (CLEO Collaboration), Phys. Rev. D **30,** 1433 (1984).

[44] T. Bowcock *et al.* (CLEO Collaboration), Phys. Rev. Lett. **58,** 307 (1987); I. C. Brock *et al.* (CLEO Collaboration), Phys. Rev. D **43,** 1448 (1991).

TABLES

TABLE I. Quarkonium ground-state masses (in GeV/c^2) in three potentials.

Observable	QCD, Ref. [8]	Power-law, Ref. [9]	Logarithmic, Ref. [10]	Cornell, Ref. [4]
$(c\bar{c})$ 1S	3.067	3.067	3.067	3.067
ψ	3.097	3.097	3.097	3.097
η_c	2.980	2.980	2.980	2.980
$\psi - \eta_c$	0.117[a]	0.117[b]	0.117[c]	0.117[d]
$(c\bar{b})$ 1S	6.317	6.301	6.317	6.321
B_c^*	6.337	6.319	6.334	6.343
B_c	6.264	6.248	6.266	6.254
$B_c^* - B_c$	0.073	0.071	0.068	0.089
$(b\bar{b})$ 1S	9.440	9.446	9.444	9.441
Υ	9.464	9.462	9.460	9.476
η_b	9.377	9.398	9.395	9.335
$\Upsilon - \eta_b$	0.087	0.064	0.065	0.141

[a]Input value; determines $\alpha_s = 0.36$. [b]Input value; determines $\alpha_s = 0.43$. [c]Input value; determines $\alpha_s = 0.37$. [d]Input value; determines $\alpha_s = 0.31$.

TABLE II. Charmonium masses and leptonic widths in the Buchmüller-Tye potential.

Level	Mass (GeV/c^2)		Leptonic Width (keV)	
	Calculated	Observed[a]	Calculated	Observed[a]
1^1S_0 (η_c)	2.980	2.9788 ± 0.0019		
1^3S_1 (ψ/J)	3.097	$3.09688 \pm 0.00001 \pm 0.00006$[b]	8.00	4.72 ± 0.35
2^3P_0 (χ_{c0})	3.436	3.4151 ± 0.0010		
2^3P_1 (χ_{c1})	3.486	$3.51053 \pm 0.00004 \pm 0.00012$[b]		
2^3P_2 (χ_{c2})	3.507	$3.55615 \pm 0.00007 \pm 0.00012$[b]		
2^1P_1 (h_c)	3.493	$3.5262 \pm 0.00015 \pm 0.0002$[c]		
2^1S_0 (η_c')	3.608			
2^3S_1 (ψ')	3.686	3.68600 ± 0.00010	3.67	2.14 ± 0.21

[a]See Ref. [1]. [b]See Ref. [21]. [c]See Ref. [22].

TABLE III. $b\bar{b}$ masses and leptonic widths in the Buchmüller-Tye potential.

Level	Mass (GeV/c^2)		Leptonic Width (keV)	
	Calculated	Observed[a]	Calculated	Observed[a]
1^1S_0 (η_b)	9.377			
1^3S_1 (Υ)	9.464	9.46032 ± 0.00022	1.71	1.34 ± 0.04
2^3P_0 (χ_{b0})	9.834	9.8598 ± 0.0013		
2^3P_1 (χ_{b1})	9.864	9.8919 ± 0.0007		
2^3P_2 (χ_{b2})	9.886	9.9132 ± 0.0006		
2^1P_1 (h_b)	9.873			
2^1S_0 (η_b')	9.963			
2^3S_1 (Υ')	10.007	10.02330 ± 0.00031	0.76	0.586 ± 0.029
3^3D_1	10.120			
3^3D_2	10.126			
3^3D_3	10.130			
3^1D_2	10.127			
3^3P_0 (χ_{b0})	10.199	10.2320 ± 0.0007		
3^3P_1 (χ_{b1})	10.224	10.2549 ± 0.0006		
3^3P_2 (χ_{b2})	10.242	10.26835 ± 0.00057		
3^1P_1 (h_b)	10.231			
3^1S_0	10.298			
3^3S_1	10.339	10.3553 ± 0.0005	0.55	0.44 ± 0.03
4^1S_0	10.573			
4^3S_1	10.602	10.5800 ± 0.0035		

[a]See Ref. [1].

TABLE IV. $c\bar{b}$ masses (in GeV/c^2) in the Buchmüller-Tye potential.

Level	Calculated Mass	Eichten & Feinberg[a]	Gershteĭn et al.[b]	Chen & Kuang[c]
1^1S_0 (B_c)	6.264	6.243	6.246	6.310
1^3S_1 (B_c^*)	6.337	6.339	6.329	6.355
2^3P_0	6.700	6.697	6.645	6.728
$2\ 1^{+\prime}$	6.736	6.740	6.741	6.760
$2\ 1^{+}$	6.730	6.719	6.682	6.764
2^3P_2	6.747	6.750	6.760	6.773
2^1S_0	6.856	6.969	6.863	6.890
2^3S_1	6.899	7.022	6.903	6.917
3^3D_1	7.012			
3^3D_2	7.012			
3^3D_3	7.005		(7.008)	
3^1D_2	7.009			
3^3P_0	7.108		7.067	7.134
$3\ 1^{+\prime}$	7.142		7.129	7.159
$3\ 1^{+}$	7.135		7.099	7.160
3^3P_2	7.153		7.143	7.166
3^1S_0	7.244		(7.327)	
3^3S_1	7.280			
4^1S_0	7.562			
4^3S_1	7.594			

[a]See Ref. [14]. [b]See Ref. [27]. [c]See Ref. [28]; the masses correspond to Potential I with $\Lambda_{\overline{\rm MS}} = 150$ MeV.

TABLE V. Radial wave functions at the origin and related quantities for $c\bar{b}$ mesons.

Level	$\|R_{n\ell}^{(\ell)}(0)\|^2$			
	QCD, Ref. [8]	Power-law, Ref. [9]	Logarithmic, Ref. [10]	Cornell, Ref. [4]
1S	1.642 GeV^3	1.710 GeV^3	1.508 GeV^3	3.102 GeV^3
2P	0.201 GeV^5	0.327 GeV^5	0.239 GeV^5	0.392 GeV^5
2S	0.983 GeV^3	0.950 GeV^3	0.770 GeV^3	1.737 GeV^3
3D	0.055 GeV^7	0.101 GeV^7	0.055 GeV^7	0.080 GeV^7
3P	0.264 GeV^5	0.352 GeV^5	0.239 GeV^5	0.531 GeV^5
3S	0.817 GeV^3	0.680 GeV^3	0.563 GeV^3	1.427 GeV^3

TABLE VI. Statistical Factor $\mathcal{S}_{if}$ for ${}^3\mathrm{P}_J \to {}^3\mathrm{D}_{J'} + \gamma$ Transitions.

J	J'	$\mathcal{S}_{if}$
0	1	2
1	1	1/2
1	2	9/10
2	1	1/50
2	2	9/50
2	3	18/25

TABLE VII. E1 Transition Rates in the $c\bar{b}$ System.

Transition	Photon energy (MeV)	$\langle f\|r\|i\rangle$ (GeV^{-1})	$\Gamma(i \to f+\gamma)$ (keV)
$2^3P_2 \to 1^3S_1 + \gamma$	397	1.714	112.6
$2(1^+) \to 1^3S_1 + \gamma$	382	1.714	99.5
$2(1^+) \to 1^1S_0 + \gamma$	450	1.714	0.0
$2(1^{+\prime}) \to 1^3S_1 + \gamma$	387	1.714	0.1
$2(1^{+\prime}) \to 1^1S_0 + \gamma$	455	1.714	56.4
$2^3P_0 \to 1^3S_1 + \gamma$	353	1.714	79.2
$2^3S_1 \to 2^3P_2 + \gamma$	151	-2.247	17.7
$2^3S_1 \to 2(1^+) + \gamma$	167	-2.247	14.5
$2^3S_1 \to 2(1^{+\prime}) + \gamma$	161	-2.247	0.0
$2^3S_1 \to 2^3P_0 + \gamma$	196	-2.247	7.8
$2^1S_0 \to 2(1^+) + \gamma$	125	-2.247	0.0
$2^1S_0 \to 2(1^{+\prime}) + \gamma$	119	-2.247	5.2
$3^3D_3 \to 2^3P_2 + \gamma$	258	2.805	98.7
$3^3D_2 \to 2^3P_2 + \gamma$	258	2.805	24.7
$3^3D_2 \to 2(1^+) + \gamma$	274	2.805	88.8
$3^3D_2 \to 2(1^{+\prime}) + \gamma$	268	2.805	0.1
$3^3D_1 \to 2^3P_2 + \gamma$	258	2.805	2.7
$3^3D_1 \to 2(1^+) + \gamma$	274	2.805	49.3
$3^3D_1 \to 2(1^{+\prime}) + \gamma$	268	2.805	0.0
$3^3D_1 \to 2^3P_0 + \gamma$	302	2.805	88.6
$3^1D_2 \to 2(1^{+\prime}) + \gamma$	268	2.805	92.5
$3^3P_2 \to 1^3S_1 + \gamma$	770	0.304	25.8
$3^3P_2 \to 2^3S_1 + \gamma$	249	2.792	73.8
$3^3P_2 \to 3^3D_3 + \gamma$	142	-2.455	17.8
$3^3P_2 \to 3^3D_2 + \gamma$	142	-2.455	3.2
$3^3P_2 \to 3^3D_1 + \gamma$	142	-2.455	0.2
$3(1^+) \to 1^3S_1 + \gamma$	754	0.304	22.1
$3(1^+) \to 2^3S_1 + \gamma$	232	2.792	54.3
$3(1^+) \to 3^3D_2 + \gamma$	125	-2.455	9.8
$3(1^+) \to 3^3D_1 + \gamma$	125	-2.455	0.3
$3(1^{+\prime}) \to 1^3S_1 + \gamma$	760	0.304	2.1
$3(1^{+\prime}) \to 2^3S_1 + \gamma$	239	2.792	5.4
$3(1^{+\prime}) \to 3^3D_2 + \gamma$	131	-2.455	11.5
$3(1^{+\prime}) \to 3^3D_1 + \gamma$	131	-2.455	0.4
$3^3P_0 \to 1^3S_1 + \gamma$	729	0.304	21.9
$3^3P_0 \to 2^3S_1 + \gamma$	205	2.792	41.2
$3^3P_0 \to 3^3D_1 + \gamma$	98	-2.455	6.9

TABLE VIII. M1 Transition Rates in the $c\bar{b}$ System.

Transition	Photon energy (MeV)	$\langle f \vert j_0(kr/2) \vert i \rangle$	$\Gamma(i \to f + \gamma)$ (keV)
$2^3S_1 \to 2^1S_0 + \gamma$	43	0.9990	0.0289
$2^3S_1 \to 1^1S_0 + \gamma$	606	0.0395	0.1234
$2^1S_0 \to 1^3S_1 + \gamma$	499	0.0265	0.0933
$1^3S_1 \to 1^1S_0 + \gamma$	72	0.9993	0.1345

TABLE IX. The relative rates for the allowed two-pion E1–E1 transitions between spin-triplet states and spin-singlet states. The reduced rates are denoted by $A_k(\ell', \ell)$ where k is the rank of the irreducible tensor for gluon emission and ℓ' and ℓ are the orbital angular momenta of the initial and final states respectively.

Transition	Rate	$c\bar{b}$ Estimate (keV)[a]
$3^3P_2 \to 2^3P_2 + \pi\pi$	$A_0(1,1)/3 + A_1(1,1)/4 + 7A_2(1,1)/60$	1.4
$3^3P_2 \to 2^3P_1 + \pi\pi$	$A_1(1,1)/12 + 3A_2(1,1)/20$	0.03
$3^3P_2 \to 2^3P_0 + \pi\pi$	$A_2(1,1)/15$	0.01
$3^3P_1 \to 2^3P_2 + \pi\pi$	$5A_1(1,1)/36 + A_2(1,1)/4$	0.05
$3^3P_1 \to 2^3P_1 + \pi\pi$	$A_0(1,1)/3 + A_1(1,1)/12 + A_2(1,1)/12$	0.02
$3^3P_1 \to 2^3P_0 + \pi\pi$	$A_1(1,1)/9$	0
$3^3P_0 \to 2^3P_2 + \pi\pi$	$A_2(1,1)/3$	0.07
$3^3P_0 \to 2^3P_1 + \pi\pi$	$A_1(1,1)/3$	0
$3^3P_0 \to 2^3P_0 + \pi\pi$	$A_0(1,1)/3$	1.4
$3^3D_{J'} \to 1^3S_1 + \pi\pi$	$A_2(2,0)/5$	32 ± 11
$2^3S_1 \to 1^3S_1 + \pi\pi$	$A_0(0,0)$	50 ± 7
$3^1P_1 \to 2^1P_1 + \pi\pi$	$A_0(1,1)/3 + A_1(1,1)/3 + A_2(1,1)/3$	1.4
$3^1D_2 \to 1^1S_0 + \pi\pi$	$A_2(2,0)/5$	32 ± 11
$2^1S_0 \to 1^1S_0 + \pi\pi$	$A_0(0,0)$	50 ± 7

[a]Sum of $\pi^+\pi^-$ and $\pi^0\pi^0$.

TABLE X. Estimated rates for two-pion E1–E1 transitions between $c\bar{b}$ levels, scaled from $c\bar{c}$ and $b\bar{b}$ measurements and calculations.

Transition	$(Q\bar{Q})$ rate (keV)	$\langle r^2(c\bar{b})\rangle/\langle r^2(Q\bar{Q})\rangle$	Reduced rate $(c\bar{b})$ (keV)
	$(b\bar{b}):\ 11.7 \pm 2.2^{\rm a}$	1.99	$A_0(0,0) = 40 \pm 8$
$2^3S_1 \to 1^3S_1 + \pi\pi$	$(c\bar{c}):\ 141 \pm 27^{\rm a}$	0.70	$A_0(0,0) = 69 \pm 13$
	Mean		$A_0(0,0) = 50 \pm 7$
	$(c\bar{c}):\ 37 \pm 17 \pm 8^{\rm b}$		$A_2(2,0) = 137 \pm 70$
$3^3D_1 \to 1^3S_1 + \pi\pi$	$(c\bar{c}):\ 55 \pm 23 \pm 11^{\rm c}$	0.72	$A_2(2,0) = 204 \pm 94$
	Mean: 43 ± 15		$A_2(2,0) = 160 \pm 56$
$3^3P_0 \to 2^3P_0 + \pi\pi$	$(b\bar{b}):\ 0.4^{\rm d}$	1.88	$A_0(1,1) = 4.2$
$3^3P_2 \to 2^3P_1 + \pi\pi$	$(b\bar{b}):\ 0.01^{\rm d}$	1.88	$A_2(1,1) = 0.2$

[a]Particle Data Group average [1]. [b]Measured by the Crystal Ball [38] and Mark II [39] Collaborations. [c]Measured by the Mark III Collaboration [40]. [d]Calculated by Kuang and Yan [34] using the Buchmüller-Tye potential [8].

TABLE XI. Total widths and branching fractions of $c\bar{b}$ levels.

Decay Mode		Branching Fraction (percent)
	$1^3\mathrm{S}_1$: $\Gamma = 0.135$ keV	
$1^1\mathrm{S}_0 + \gamma$		100
	$2^1\mathrm{S}_0$: $\Gamma = 55$ keV	
$1^1\mathrm{S}_0 + \pi\pi$		91
$2(1^{+\prime}) + \gamma$		9
	$2^3\mathrm{S}_1$: $\Gamma = 90$ keV	
$1^3\mathrm{S}_1 + \pi\pi$		55
$2^3\mathrm{P}_2 + \gamma$		20
$2(1^+) + \gamma$		16
$2^3\mathrm{P}_0 + \gamma$		9
	$2^3\mathrm{P}_0$: $\Gamma = 79$ keV	
$1^3\mathrm{S}_1 + \gamma$		100
	$2(1^+)$: $\Gamma = 100$ keV	
$1^3\mathrm{S}_1 + \gamma$		100
	$2(1^{+\prime})$: $\Gamma = 56$ keV	
$1^1\mathrm{S}_0 + \gamma$		100
	$2^3\mathrm{P}_2$: $\Gamma = 113$ keV	
$1^3\mathrm{S}_1 + \gamma$		100
	$3^3\mathrm{D}_1$: $\Gamma = 173$ keV	
$1^3\mathrm{S}_1 + \pi\pi$		18
$2^3\mathrm{P}_2 + \gamma$		2
$2(1^+) + \gamma$		29
$2^3\mathrm{P}_0 + \gamma$		51
	$3^3\mathrm{D}_2$: $\Gamma = 146$ keV	
$1^3\mathrm{S}_1 + \pi\pi$		22
$2^3\mathrm{P}_2 + \gamma$		17
$2(1^+) + \gamma$		61
	$3^3\mathrm{D}_3$: $\Gamma = 131$ keV	
$1^3\mathrm{S}_1 + \pi\pi$		24
$2^3\mathrm{P}_2 + \gamma$		76
	$3^1\mathrm{D}_2$: $\Gamma = 124$ keV	
$1^1\mathrm{S}_0 + \pi\pi$		26
$2(1^{+\prime}) + \gamma$		74
	$3^3\mathrm{P}_0$: $\Gamma = 71$ keV[a]	
$2^3\mathrm{P}_0 + \pi\pi$		2
$1^3\mathrm{S}_1 + \gamma$		31
$2^3\mathrm{S}_1 + \gamma$		57
$3^3\mathrm{D}_1 + \gamma$		10
	$3(1^+)$: $\Gamma = 86$ keV[a]	
$1^3\mathrm{S}_1 + \gamma$		26
$2^3\mathrm{S}_1 + \gamma$		63
$3^3\mathrm{D}_2 + \gamma$		11
	$3(1^{+\prime})$: $\Gamma = 21$ keV[a]	
$2(1^{+\prime}) + \pi\pi$		7
$1^3\mathrm{S}_1 + \gamma$		10
$2^3\mathrm{S}_1 + \gamma$		26
$3^3\mathrm{D}_2 + \gamma$		55
	$3^3\mathrm{P}_2$: $\Gamma = 122$ keV[a]	
$2^3\mathrm{P}_2 + \pi\pi$		1
$1^3\mathrm{S}_1 + \gamma$		21
$2^3\mathrm{S}_1 + \gamma$		60
$3^3\mathrm{D}_3 + \gamma$		15
$3^3\mathrm{D}_2 + \gamma$		3

[a]Should this state lie above flavor threshold, dissociation into BD will dominate over the tabulated decay modes.

FIGURES

FIG. 1. The spectrum of $c\bar{b}$ states.

FIG. 2. Normalized dipion mass spectrum for the transition $2^3\mathrm{S}_1 \to 1^3\mathrm{S}_1 + \pi\pi$ in the ψ (dashed curve), B_c (solid curve), and Υ (dotted curve) families.

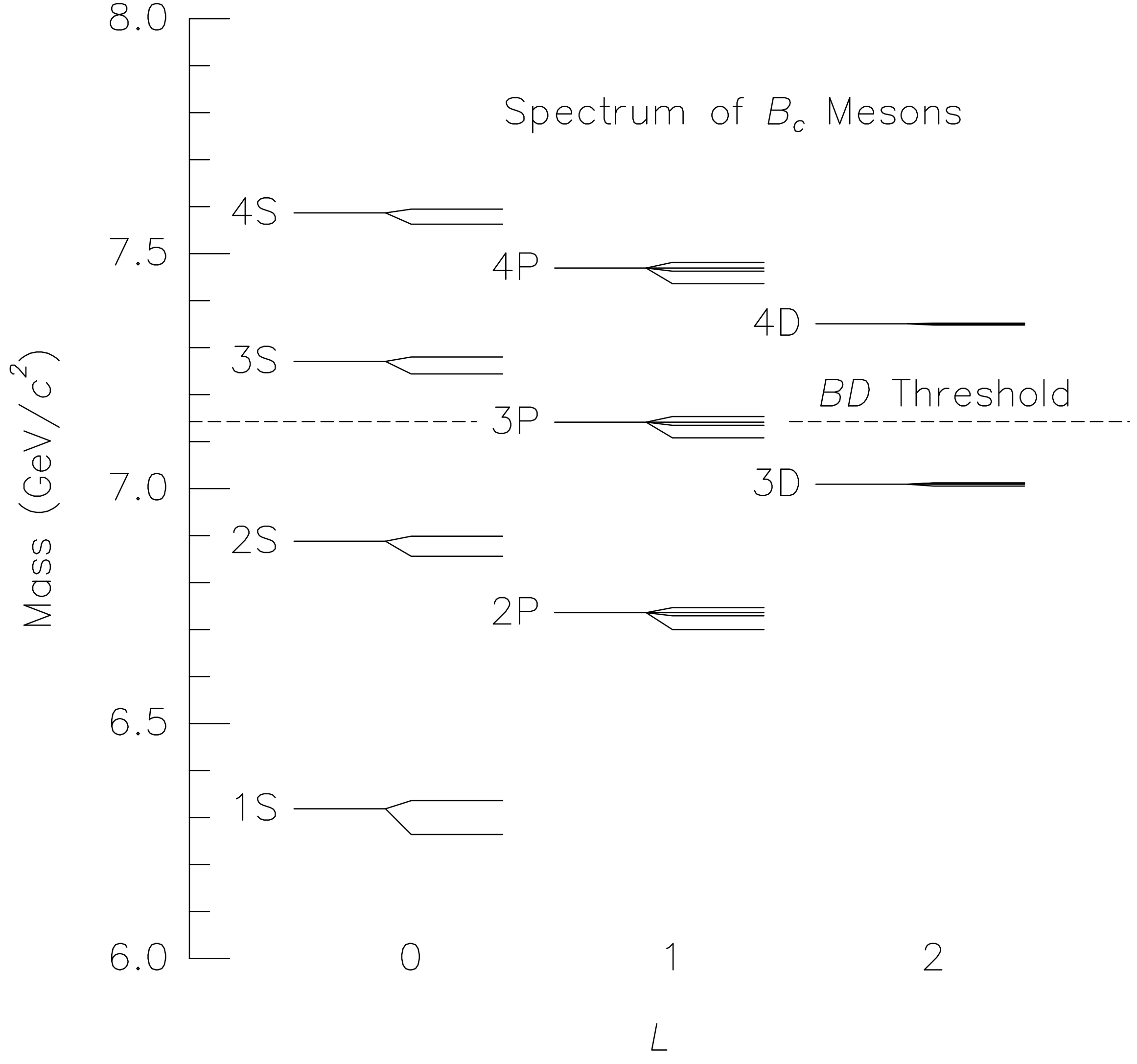
Spectrum of B_c Mesons
Mass (GeV/c^2)
8.0
7.5
7.0
6.5
6.0
4S
3S
2S
1S
4P
3P
2P
4D
3D
BD Threshold
0
1
2
L

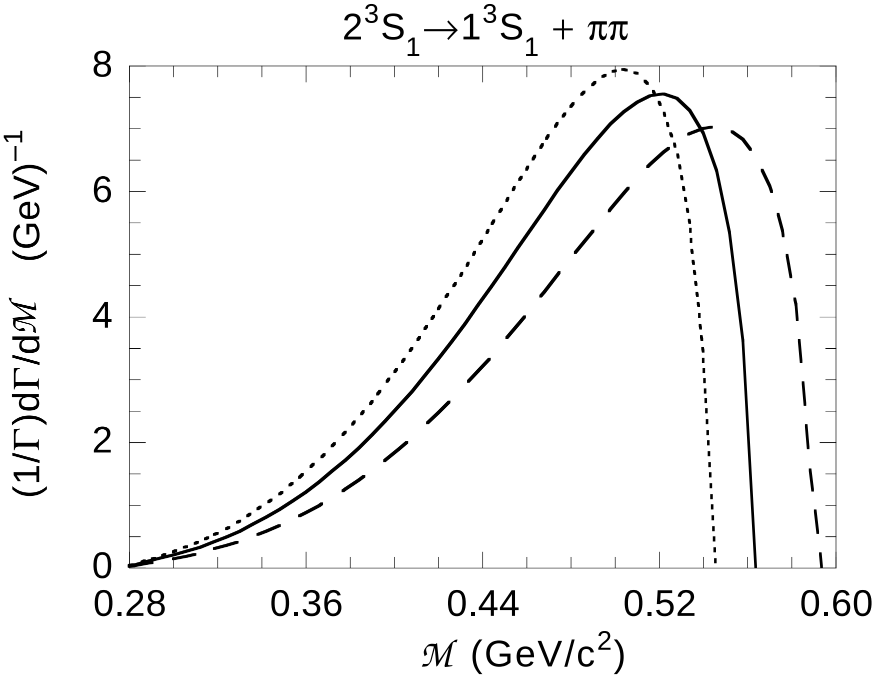

$2^3S_1 \rightarrow 1^3S_1 + \pi\pi$
$(1/\Gamma)d\Gamma/d\mathcal{M}$ (GeV)$^{-1}$
0
2
4
6
8
0.28
0.36
0.44
0.52
0.60
$\mathcal{M}$ (GeV/c^2)